Hindawi Publishing Corporation
Advances in High Energy Physics
Volume 2014, Article ID 675192, 10 pages
http://dx.doi.org/10.1155/2014/675192

Research Article

Emission of Protons and Charged Pions in p + Cu and p + Pb Collisions at 3, 8, and 15 GeV/c

J. H. Kang,[1] Y. C. Qian,[2] B. C. Li,[2] and S. W. Wu[2]

[1] *Institute of Theoretical Physics, Shanxi University, Taiyuan 030006, China*
[2] *College of Physics and Electronic Engineering, Shanxi University, Taiyuan 030000, China*

Correspondence should be addressed to B. C. Li; bcli_th@yeah.net

Received 6 May 2014; Accepted 6 July 2014; Published 20 July 2014

Academic Editor: Chen Wu

We present an analysis of proton and charged pion transverse momentum spectra of p+Cu and p+Pb reactions at 3, 8, and 15 GeV/c in the framework of a multisource thermal model. The spectra are compared closely with the experimental data of HARP-CDP at all angular intervals. The result shows that the widths of the particle distributions in both p + Cu and p + Pb collisions decrease with increasing the angle for the same incident momentum.

1. Introduction

The relativistic heavy ion collider (RHIC) [1, 2] in the United States and the large hadron collider (LHC) [3] in Switzerland have been built, respectively. Much higher energy collisions can lead to a new significant extension of the kinematic range in transverse momentum. The collisions bring valuable information of quark gluon plasma (QGP) at high energy due to high temperature and density [4, 5]. The state is a thermalized system consisting of strong coupled quarks and gluons in a very small region. This matter is only created for the briefest of instants, and then the fireball cools down and hadronizes into hadrons. So, we cannot observe the QGP directly in the existing laboratory conditions. However, we can extract a judgment of the creation of the quark matter by measuring and analyzing the spectra of identified particles produced after thermal freeze-out in heavy ion collisions.

In a very early stage of the collision, the energy density is expected to be sufficient to dissolve normal nuclear matter into a phase of quark matter, which exists for only a short time before the fireball cools down and the process of hadronization takes place. High-energy collisions provide an excellent probe of the quark matter. Properties of QGP will be probed further in LHC at the European Organization for Nuclear Research (CERN) [6]. The proton-nucleus collisions are important in experimental programmes performed in the LHC [7] because they not only provide baseline measurements for the nucleus-nucleus collisions but also help us better understand fundamental features of quantum chromodynamics (QCD) [8]. The transverse momentum spectra of final-state particles can give some important information of the matter created in high-energy collisions. In this paper, we use a multisource thermal model to study transverse momentum spectra of protons and charged pions produced in p+Cu and p+Pb collisions at 3, 8, and 15 GeV/c, recently measured in the Hadron Production Experiment (HARP) at the CERN [9].

2. Distribution of Transverse Momentum

In a framework of the multisource thermal model [10, 11], identified fragments or particles emit isotropically from different emission sources in the collisions. In order to deal conveniently with the relation between the sources and particles, we split the sources into k groups in accordance with kinetic laws and geometrical positions. For the mth source in the nth group, its share of the transverse momentum spectrum of the final-state particles is given by

$$f_{mn}\left(P_{\mathrm{T}mn}\right) = \frac{1}{\langle P_{\mathrm{T}mn}\rangle} \exp\left(-\frac{P_{\mathrm{T}mn}}{\langle P_{\mathrm{T}mn}\rangle}\right), \quad (1)$$

Table 1: Values of $\langle P_{\mathrm{Tm}1}\rangle$, c_1 taken in the fits of Figures 1 and 2.

Figure 1	$\langle P_{\mathrm{Tm}1}\rangle$	c_1	χ^2/dof	Figure 2	$\langle P_{\mathrm{Tm}1}\rangle$	c_1	χ^2/dof
(a_1)	0.19	1	0.03	(a_1)	0.09	1	0.19
(a_2)	0.18	1	0.03	(a_2)	0.14	1	0.23
(a_3)	0.18	1	0.06	(a_3)	0.14	1	0.14
(b_1)	0.15	1	0.20	(b_1)	0.09	1	0.54
(b_2)	0.14	1	0.08	(b_2)	0.13	1	0.27
(b_3)	0.16	1	0.07	(b_3)	0.13	1	0.29
(c_1)	0.08	1	0.14	(c_1)	0.05	1	0.83
(c_2)	0.09	1	0.02	(c_2)	0.07	1	0.51
(c_3)	0.10	1	0.15	(c_3)	0.07	1	1.20

Table 2: Values of $\langle P_{\mathrm{Tm}1}\rangle$, c_1 taken in the fits of Figures 3 and 4.

Figure 3	$\langle P_{\mathrm{Tm}1}\rangle$	c_1	χ^2/dof	Figure 4	$\langle P_{\mathrm{Tm}1}\rangle$	c_1	χ^2/dof
(a_1)	0.11	1	0.20	(a_1)	0.17	1	0.05
(a_2)	0.16	1	0.05	(a_2)	0.16	1	0.13
(a_3)	0.16	1	0.09	(a_3)	0.17	1	0.13
(b_1)	0.11	1	1.00	(b_1)	0.14	1	0.16
(b_2)	0.13	1	0.19	(b_2)	0.13	1	0.52
(b_3)	0.13	1	0.49	(b_3)	0.15	1	0.03
(c_1)	0.05	1	1.49	(c_1)	0.08	1	0.12
(c_2)	0.08	1	0.85	(c_2)	0.09	1	—
(c_3)	0.08	1	0.66	(c_3)	0.10	1	—

where

$$\langle P_{\mathrm{Tm}n}\rangle = \int P_{\mathrm{Tm}n} f_{mn}\left(P_{\mathrm{Tm}n}\right) dP_{\mathrm{Tm}n} \tag{2}$$

is the mean value of the transverse momentum which comes from the mth source in the nth group. According to statistical properties of the model, we have

$$\langle P_{T1n}\rangle = \langle P_{T2n}\rangle = \cdots = \left\langle P_{Tl_n n}\right\rangle. \tag{3}$$

l_n indicates the source number in the nth group. By computing convolution of the l_n exponential functions equation (1), the total share of the nth group for the transverse momentum P_T distribution is obtained as

$$f_n\left(P_T\right) = \frac{P_T^{\,l_n-1}}{\left(l_n-1\right)!\langle P_{\mathrm{Tm}n}\rangle^{l_n}} \exp\left(-\frac{P_T}{\langle P_{\mathrm{Tm}n}\rangle}\right). \tag{4}$$

It is an Erlang distribution. Then, the transverse momentum distribution from the k groups is given by

$$f\left(P_T\right) = \sum_{n=1}^{k} c_n f_n\left(P_T\right), \tag{5}$$

where c_n characterizes how large the contribution of the sources in the nth group is. Equation (5) is known as a multicomponent Erlang distribution. To simplify the calculation, the Monte Carlo method is used to calculate the transverse momentum spectra. With (1) and (4), the transverse momentum distribution is

$$P_{\mathrm{Tm}n} = -\langle P_{\mathrm{Tm}n}\rangle \ln R_{mn}, \tag{6}$$

$$P_T = -\sum_{m=1}^{l_n} \langle P_{\mathrm{Tm}n}\rangle \ln R_{mn}, \tag{7}$$

where R_{mn} is a random number in [0, 1].

3. Comparison with HARP Results

Figures 1, 2, and 3 present the transverse momentum spectra of p, π^-, and π^+ in p + Cu collisions at 3, 8, and 15 GeV/c at different angular intervals, respectively. From the first column to the third column in the figures, the momenta of incident protons are 3, 8, and 15 GeV/c, respectively. And from the first row to the third row in the figures, the angular intervals are 30°–40°, 60°–75°, and 105°–125°, separately. The symbols indicate the experimental data [9] in the HARP experiment at the CERN. The solid lines are the results of the multisource thermal model. The parameters and χ^2 per degree of freedom (dof) are given in Tables 1 and 2. In the 30°–40° angular interval, the value of $\langle P_{\mathrm{Tm}1}\rangle$ for the p production at 8 GeV/c incident momentum is equal to that at the 15 GeV/c. Moreover, for π^-, the $\langle P_{\mathrm{Tm}1}\rangle$ at 8 GeV/c and 15 GeV/c are the same in the three angular intervals. So is it for π^+. In the calculation, one group with two sources is selected. We see that the model can successfully describe the experimental data. From the figures and the tables, it is

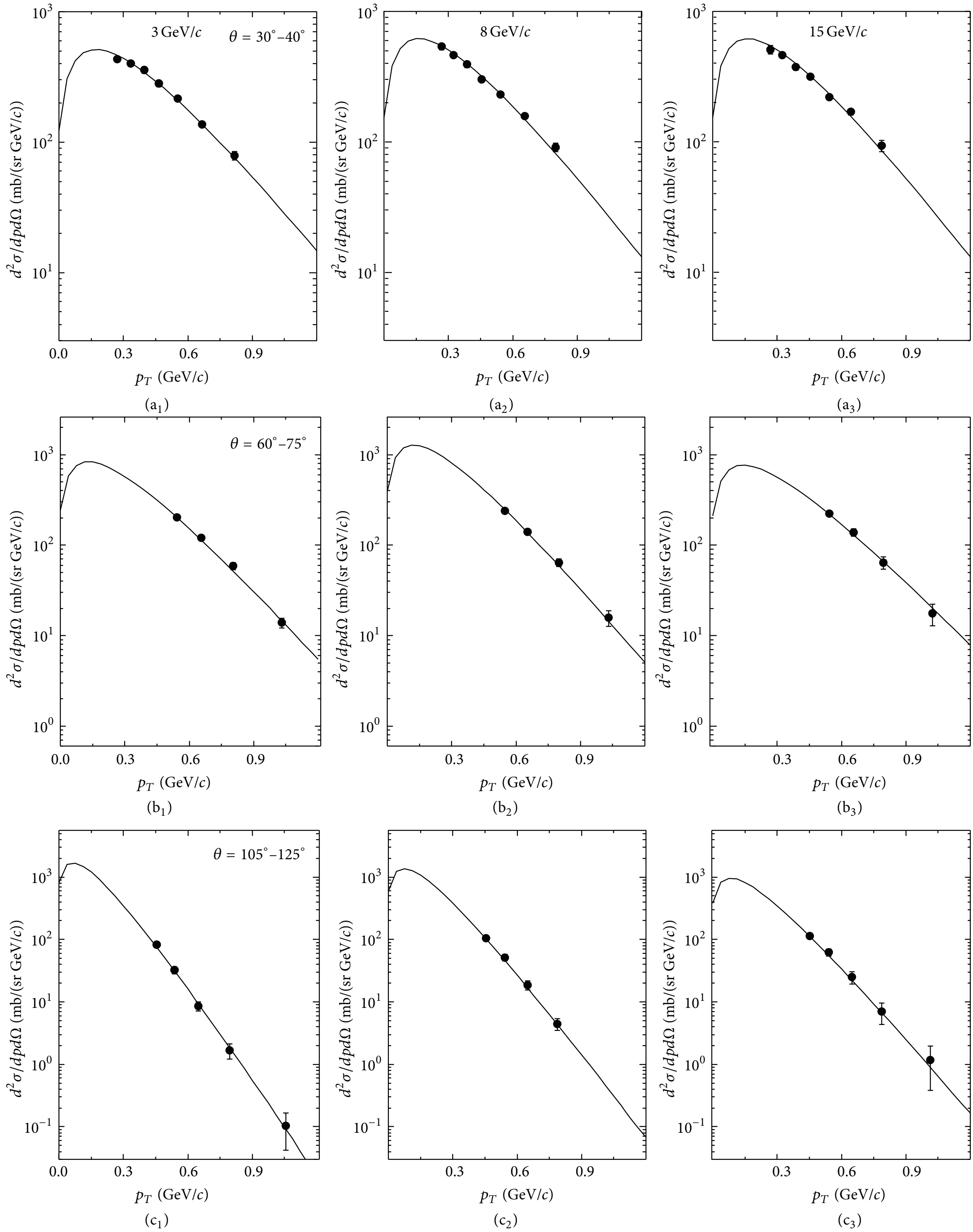

FIGURE 1: Transverse momentum of protons produced in p + Cu collisions at 3, 8, and 15 GeV/c. The angular bins are 30°–40°, 60°–75°, and 105°–125°, respectively. The circles indicate the experimental data [9] and the curves indicate the results of the model.

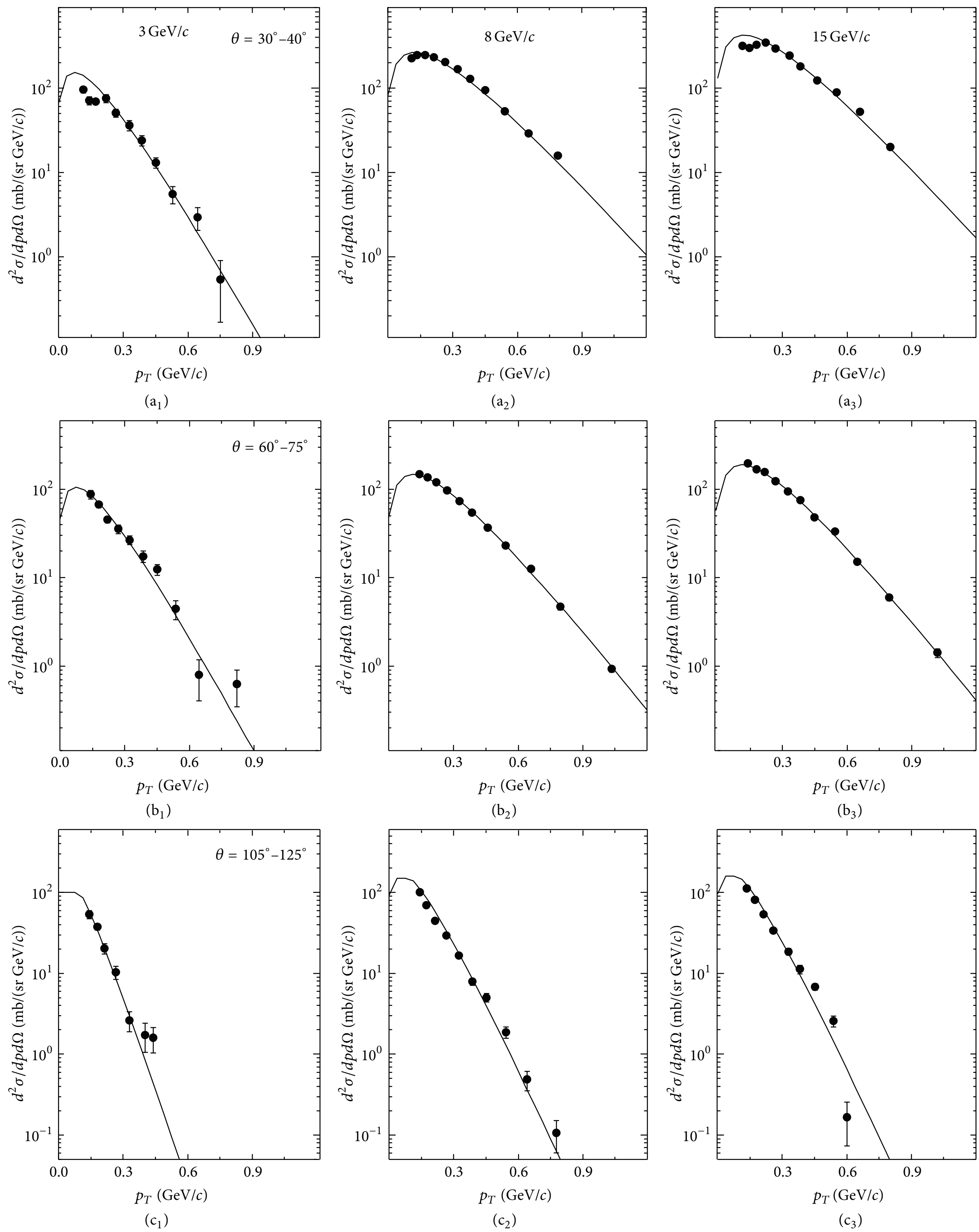

FIGURE 2: The same as Figure 1, but for π^-.

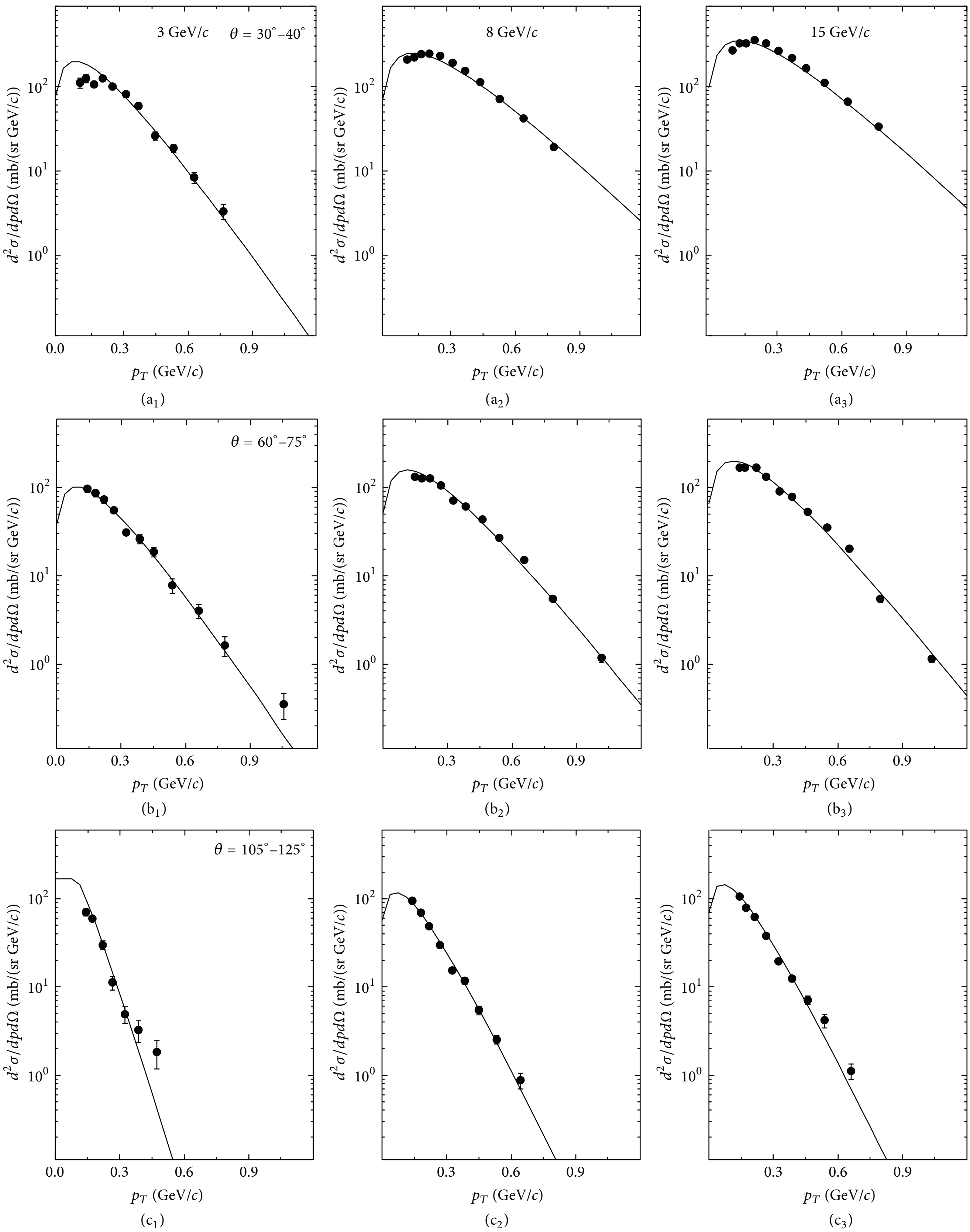

Figure 3: The same as Figure 1, but for π^+.

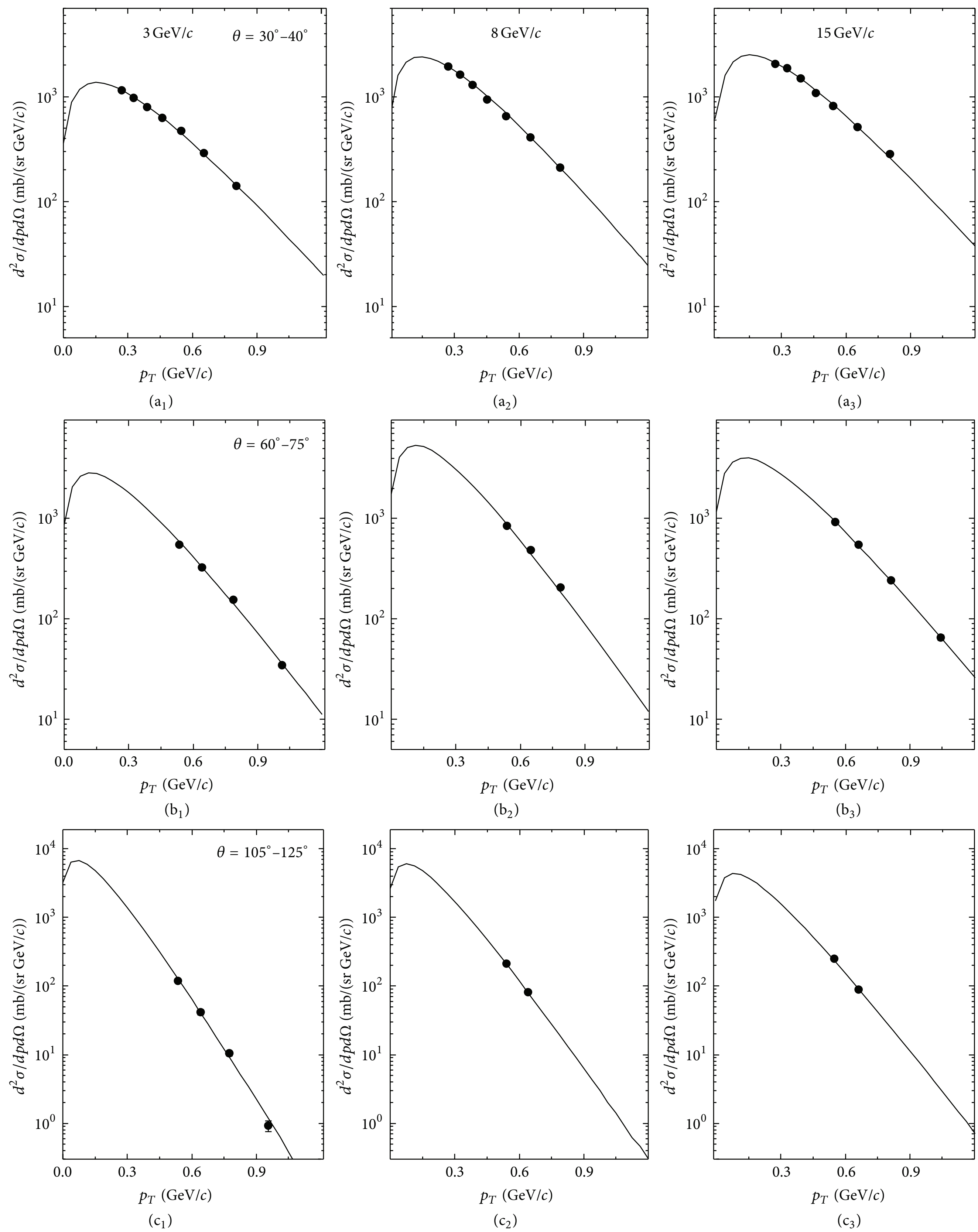

FIGURE 4: Transverse momentum of protons produced in p + Pb collisions at 3, 8, and 15 GeV/c. The angular bins are 30°–40°, 60°–75°, and 105°–125°, respectively. The circles indicate the experimental data [9] and the curves indicate the results of the model.

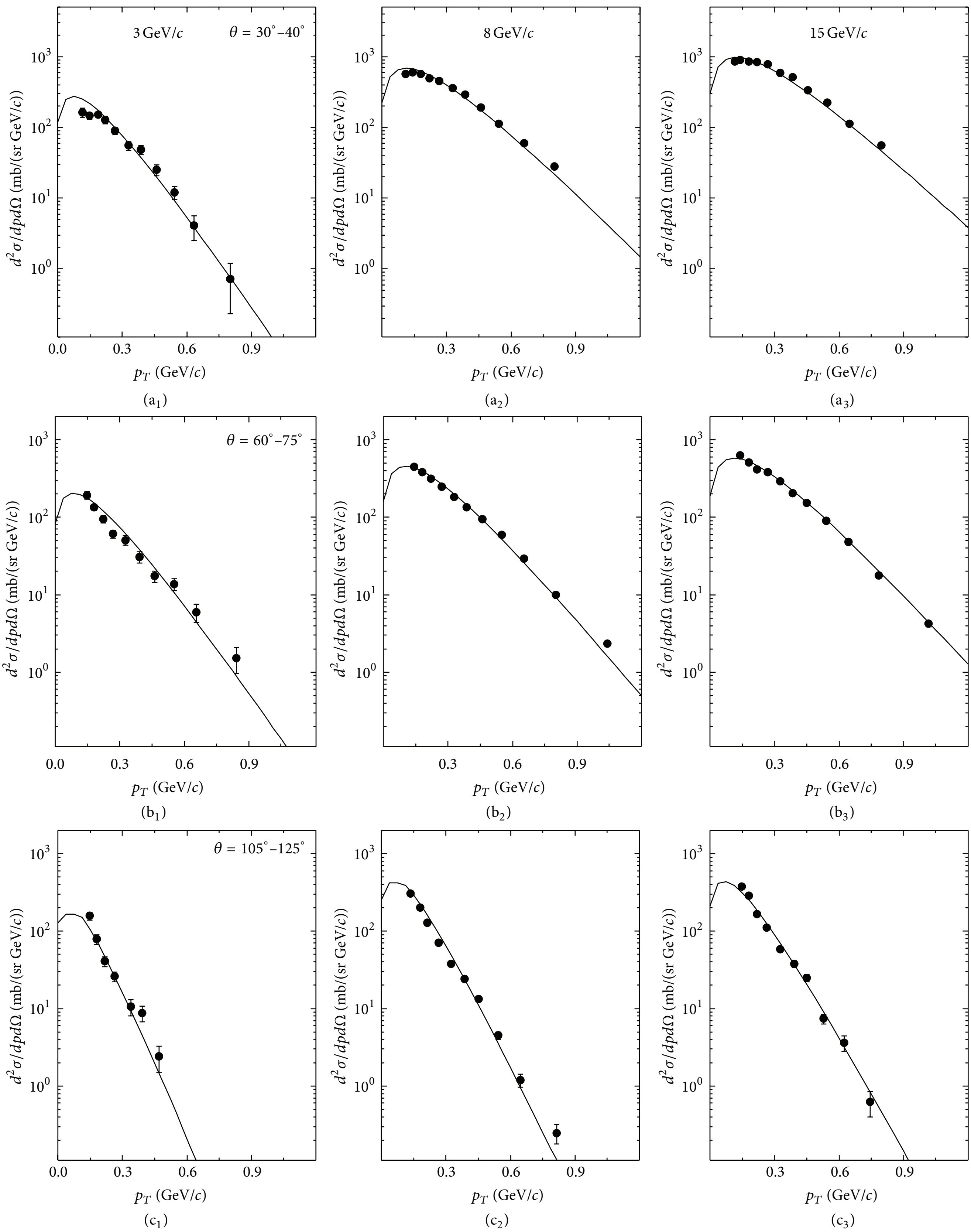

FIGURE 5: The same as Figure 4, but for π^-.

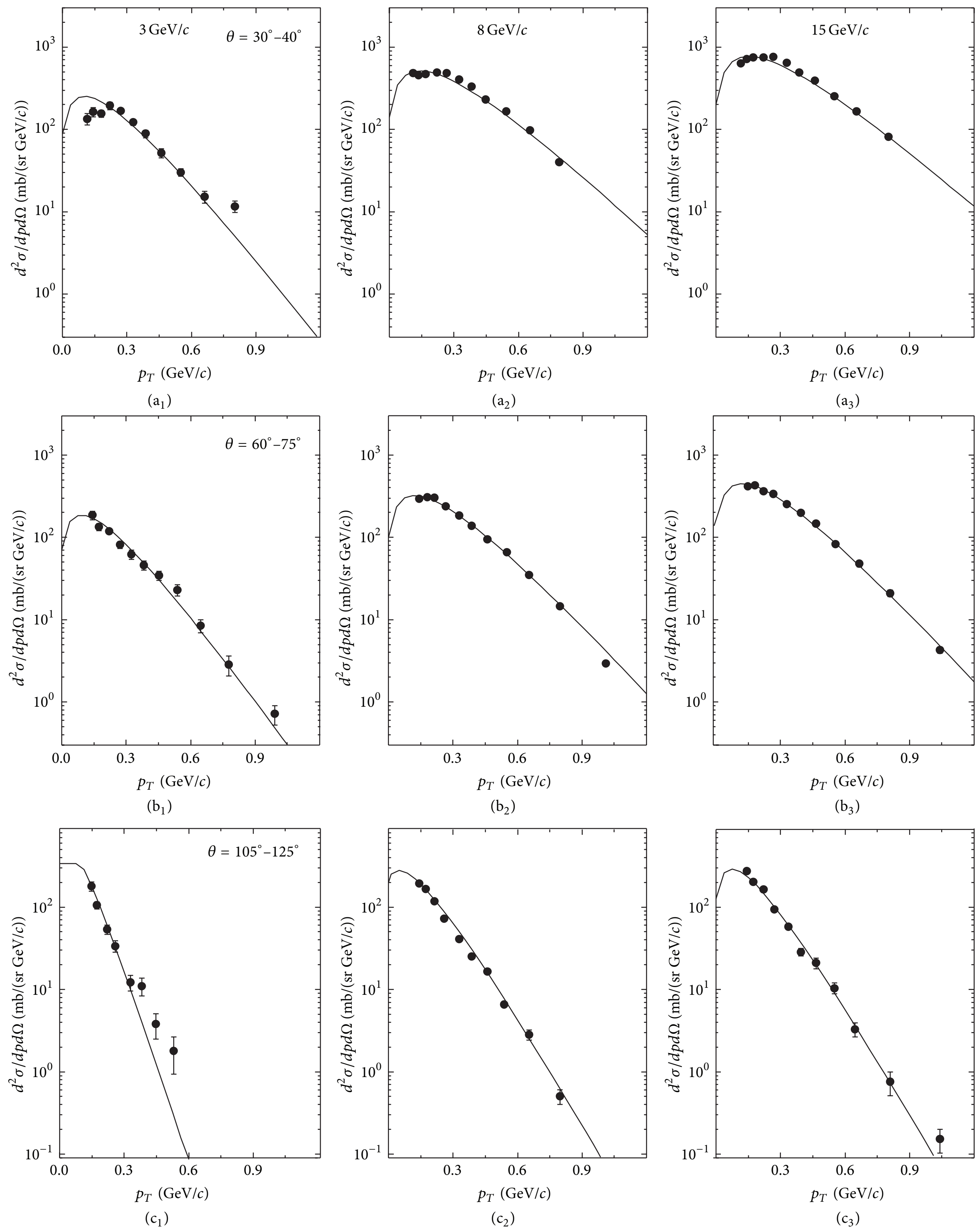

Figure 6: The same as Figure 4, but for π^+.

Table 3: Values of $\langle P_{Tm1} \rangle$, c_1 taken in the fits of Figures 5 and 6.

Figure 5	$\langle P_{Tm1} \rangle$	c_1	χ^2/dof	Figure 6	$\langle P_{Tm1} \rangle$	c_1	χ^2/dof
(a_1)	0.09	1	0.18	(a_1)	0.12	1	0.56
(a_2)	0.13	1	0.31	(a_2)	0.16	1	0.22
(a_3)	0.14	1	0.20	(a_3)	0.17	1	0.11
(b_1)	0.10	1	0.62	(b_1)	0.11	1	0.55
(b_2)	0.12	1	0.75	(b_2)	0.14	1	0.35
(b_3)	0.13	1	1.26	(b_3)	0.14	1	0.15
(c_1)	0.06	1	1.12	(c_1)	0.05	1	1.73
(c_2)	0.07	1	1.33	(c_2)	0.09	1	0.95
(c_3)	0.08	1	1.63	(c_3)	0.09	1	0.45

also found that the width or the mean contribution $\langle P_{Tm1} \rangle$ of the distribution decreases with increasing the angular intervals for the same incident momentum.

Figures 4, 5, and 6 show the transverse momentum spectra of p, π^-, and π^+in p + Pb interactions at 3, 8, and 15 GeV/c with different angular bins. The symbols indicate the HARP-CDP experimental data [9] and the solid lines indicate the results of the multisource thermal model. The results of (7) are in agreement with the experimental data. The corresponding parameters and χ^2/dof are listed in Tables 2 and 3. At forward angles $\theta = 30^\circ$–40°, the values of $\langle P_{Tm1} \rangle$ are the same for proton production at 3 GeV/c incident momentum and for the 15 GeV/c. For π^+ production, the $\langle P_{Tm1} \rangle$ at 8 GeV/c and 15 GeV/c are the same at the angles of 60°–75° and 105°–125°. Like the case of p + Cu collisions, we still use a single group with two sources and the results agree well with the experimental data. At the same incident momentum, the $\langle P_{Tm1} \rangle$ decreases with the increase of the forward angles.

4. Discussion and Conclusion

In the multisource thermal model, the transverse momentum spectra of protons and charged pions produced in protons on Cu and Pb collisions at 3, 8, and 15 GeV/c in fixed angles of 30°–40°, 60°–75°, and 105°–125° are discussed. The spectra of the model are in agreement with the HARP-CDP data. The maximum value of χ^2/dof is 1.73, and the minimum value is 0.02. From the above discussions, it is seen that the distribution widths of the concerned particles in both p + Cu and p+Pb reactions decrease with increasing the angular intervals for the same incident momentum.

In the work, two sources in one group are used to study the experimental data. It implies that the final-state particles emit from two sources. The model can provide an explanation not only for one group but also for more groups. In the previous work, the model was used to investigateelliptic flows [10], particle production [11, 12], longitudinal shift in (pseudo) rapidity distributions [13, 14], and so forth. For various types of collision systems, the multicomponent Erlang distribution can fit the transverse momentum spectra. The work reveals a multisource production phenomenon in the heavy ion collisions.

Conflict of Interests

The authors declare that there is no conflict of interests regarding the publication of this paper.

Acknowledgments

This work is supported by the National Natural Science Foundation of China under Grant nos. 11247250 and 11005071 and the National Fundamental Fund of Personnel Training (no. J1103210).

References

[1] K. Adcox, S. S. Adler, and N. N. Ajitanand (PHENIX Collaboration), "Suppression of hadrons with large transverse momentum in central Au + Au collisions at $\sqrt{s_{NN}}$ = 130 GeV," *Physical Review Letters*, vol. 88, Article ID 022301, 2001.

[2] J. Adams, C. Adler, M. M. Aggarwal et al., "Azimuthal anisotropy at the relativistic heavy ion collider: the first and fourth harmonics," *Physical Review Letters*, vol. 92, Article ID 062301, 2004.

[3] K. Aamodt, A. A. Quintana, D. Adamová et al., "Centrality dependence of the charged-particle multiplicity density at midrapidity in Pb-Pb collisions at $\sqrt{s_{NN}}$ = 2.76 TeV," *Physical Review Letters*, vol. 106, Article ID 032301, 2011.

[4] P. Romatschke and U. Romatschke, "Viscosity information from relativistic nuclear collisions: how perfect is the fluid observed at RHIC?" *Physical Review Letters*, vol. 99, Article ID 172301, 2007.

[5] B. B. Abelev, J. Adam, D. Adamova (ALICE Collaboration) et al., "$\mathbf{K}^0_\mathbf{S}$ and $\mathbf{\Lambda}$ Production in Pb-Pb Collisions at $\sqrt{s_{NN}}$ = 2.76 TeV," *Physical Review Letters*, vol. 111, Article ID 222301, 2013.

[6] K. Aamodtet, B. Abelev, and A. Quintana (ALICE Collaboration), "Higher harmonic anisotropic flow measurements of charged particles in Pb-Pb collisions at $\sqrt{s_{NN}}$ = 2.76 TeV," *Physical Review Letters*, vol. 107, Article ID 032301, 2011.

[7] A. Bzdak and V. Skokov, "Decisive test of color coherence in rroton-nucleus vollisions at the LHC," *Physical Review Letters*, vol. 111, Article ID 182301, 2013.

[8] P. Bożek and W. Broniowski, "Collective dynamics in high-energy proton-nucleus collisions," *Physical Review C*, vol. 88, Article ID 014903, 2013.

[9] K. Abdel-Waged, N. Felemban, and V. V. Uzhinskii, "Geant4 hadronic cascade models analysis of proton and charged pion transverse momentum spectra from p^+ Cu and Pb collisions at 3, 8, and 15 GeV/c," *Physical Review C—Nuclear Physics*, vol. 84, no. 1, Article ID 014905, 2011.

[10] F. H. Liu, X. Y. Yin, J. L. Tian, and N. N. Abd Allah, "Charged-particle (pseudo)rapidity distributions in e^+e^-, $p\overline{p}$, and AA collisions at high energies," *Physical Review C*, vol. 69, Article ID 034905, 2004.

[11] B. C. Li, Y. Y. Fu, L. L. Wang, E. Q. Wang, and F. H. Liu, "Transverse momentum distributions of strange hadrons produced in nucleus–nucleus collisions at $\sqrt{s_{NN}}$ = 62.4," *Journal of Physics G*, vol. 39, no. 2, Article ID 025009, 2012.

[12] B.-C. Li, Y.-Z. Wang, and F.-H. Liu, "Formulation of transverse mass distributions in Au–Au collisions at $\sqrt{s_{NN}}$ = 200 GeV/nucleon," *Physics Letters B*, vol. 725, no. 4–6, pp. 352–356, 2013.

[13] B.-C. Li, Y.-Y. Fu, L.-L. Wang, and F.-H. Liu, "Transverse momentum, centrality, and participant nucleon number dependence of elliptic flow," *Advances in High Energy Physics*, vol. 2013, Article ID 908046, 7 pages, 2013.

[14] B.-C. Li, Y.-Z. Wang, F.-H. Liu, X.-J. Wen, and Y.-E. Dong, "Particle production in relativistic $pp(\overline{p})$ and AA collisions at RHIC and LHC energies with Tsallis statistics using the two-cylindrical multisource thermal model," *Physical Review D*, vol. 89, Article ID 054014, 2014.


Journal of Gravity
Journal of Photonics
The Scientific World Journal
Journal of Soft Matter
Advances in Condensed Matter Physics
Journal of Fluids
Hindawi
Submit your manuscripts at
http://www.hindawi.com
Journal of Aerodynamics
International Journal of Statistical Mechanics
International Journal of Optics
Journal of Computational Methods in Physics
Advances in High Energy Physics
Journal of Thermodynamics
Physics Research International
Advances in Astronomy
Journal of Solid State Physics
Journal of Astrophysics
International Journal of Superconductivity
Journal of Biophysics
Journal of Atomic and Molecular Physics